

Figure 2. The difference spectrum of the enzyme-bound intermediate formed during the conversion of EPSP (75 μM) to chorismate catalyzed by chorismate synthase (17 μM) at 25 $^{\circ}\text{C}$, pH 7.0. The data points are the amplitudes of traces similar to that of Figure 1b recorded at various wavelengths.

FMNH₂ is not known, and there is no consensus with respect to the overall mechanism.¹²

We report herein EPSP-induced, transient changes in the absorbance spectrum of FMNH₂ consistent with the formation of a flavin-C₄ adduct, thereby demonstrating for the first time direct involvement of redox-active FMNH₂ in the catalytic cycle.

Figure 1a shows a single-turnover experiment in which the absorbance at 400 nm was monitored using a Hi-Tech SF-51 stopped-flow spectrophotometer installed and operated in an anaerobic glovebox as previously described.¹³ A rapid increase in the absorbance, with a rise time close to the dead time of the apparatus, is followed by a decrease in absorbance that occurs with $k_{\text{obsd}} \approx 30 \text{ s}^{-1}$. The final absorbance was that observed when EPSP was omitted from syringe B when no transient absorbance changes were detected. No effects were observed when FMNH₂ was omitted or when chorismate synthase was shot against FMNH₂ alone. However, when Na₂S₂O₄ was omitted and the FMNH₂ generated photochemically in the presence of EDTA,¹⁴ absorbance changes similar to those shown in Figure 1a were observed.

Figure 1b shows the effect of increasing the EPSP concentration such that ca. 6 catalytic cycles of the enzyme (17 μM) are required for the complete conversion of EPSP to chorismate. The concentration of the intermediate is now maintained in a quasi steady state for ca. 100 ms before decaying with the same rate constant ($k_{\text{obsd}} \approx 30 \text{ s}^{-1}$).

The amplitude of the effects shown in parts a and b of Figure 1 depended in a linear manner on the FMNH₂ concentration up to a value of 20 μM with a final chorismate synthase concentration of 17 μM and a saturating EPSP concentration of 100 μM . At higher FMNH₂ concentrations, no further increase occurred (data not shown). This indicates stoichiometric, tight binding ($K < 0.5 \mu\text{M}$) of 1 equiv of FMNH₂/39K subunit of chorismate synthase. Maintaining the FMNH₂ concentration at 40 μM , with 17 μM chorismate synthase, but varying the EPSP concentration from 0 to 50 μM caused the amplitude to increase from 0 to that shown in Figure 1b. At EPSP concentrations in the range 50–100 μM , no further increase occurred. We conclude that the transient increase in absorbance at 400 nm is associated with an intermediate form of FMN that is present on the enzyme only when EPSP is being converted to chorismate. We have obtained a difference spectrum (Figure 2) for this FMN species that is not characteristic of free FMN/FMNH₂ nor of protein-bound FMN/FMNH₂ calculated from the spectra of *Klebsiella pneumoniae* flavodoxin in its oxidized and hydroquinone states.¹⁵ The essentially 0 amplitude at 580 nm indicates that FMN semiquinone¹⁴ is not formed at detectable levels.

We conclude that the FMNH₂ does not simply undergo a one- or two-electron oxidation during the catalytic cycle. The relatively small absorbance change ($\Delta\epsilon_{400} = 1.3 \text{ mM}^{-1} \text{ cm}^{-1}$) associated with the decay of the intermediate could reflect either its low steady-state concentration or its intrinsic spectral characteristics. A charge-transfer complex is a possibility, although we also note the similarity of the difference spectrum of the intermediate to that of the flavin-C₄ adduct.¹⁶ Since all four cysteinyl thiol groups predicted from the DNA sequence¹⁷ were quantitatively detected using 5,5'-dithiobis(2-nitrobenzoic acid) (DTNB)¹⁸ in 8 M urea, we do not consider that the role of FMNH₂ is to reduce a disulfide as recently reported for mercuric ion reductase.¹⁸

Acknowledgment. M.N.R. is grateful to the Science and Engineering Research Council and ICI Agrochemicals for support under the CASE awards scheme for postgraduate studies.

(16) Miller, S. M.; Massey, V.; Ballou, D.; Williams, C. H.; Distefano, M. D.; Moore, M. J.; Walsh, C. T. *Biochemistry* 1990, 29(11), 2831–2841.

(17) Charles, I. G.; Lamb, H. K.; Pickard, D.; Dougan, G.; Hawkins, A. R. *J. Gen. Microbiol.* 1990, 136, 353–358. (The gene sequence published in ref 6 (with five cysteines) is now known to be incorrect due to a frame shift error affecting the last 27 residues.)

(18) Ellman, G. L. *Arch. Biochem. Biophys.* 1959, 82, 70.

(19) Millar, G.; Anton, I. A.; Mousdale, D. M.; White, P. J.; Coggins, J. R. *Biochem. Soc. Trans.* 1986, 14, 262–263.

(20) Assayed as described in ref 8. However, these conditions are not optimal, and there is some evidence that the specific activity depends on the enzyme concentration (see ref 11). It is therefore difficult to calculate a turnover number under the conditions of the stopped-flow experiments from the steady-state assay data necessarily obtained at a much lower enzyme concentration (ca. 50 nM).

Direct Observation of MeRh(CO)₂I₃⁻: The Key Intermediate in Rhodium-Catalyzed Methanol Carbonylation

Anthony Haynes,^{1a} Brian E. Mann,^{1a} David J. Gulliver,^{1b} George E. Morris,^{1b} and Peter M. Maitlis*^{1a}

*Department of Chemistry, The University
Sheffield S3 7HF, England
Research and Development Department, BP Chemicals
Salt End, Hull HU12 8DS, England*

Received July 29, 1991

One of the most important industrial processes utilizing homogeneous transition-metal catalysis is the rhodium and iodide promoted carbonylation of methanol to acetic acid. Extensive research by the Monsanto group² and others^{3,4} indicated that the active catalyst precursor was [Rh(CO)₂I₂]⁻, A, and that the reaction proceeded as shown in Scheme 1.

In this cycle the step which determines the overall rate is the oxidative addition of MeI to Rh(CO)₂I₂⁻.⁵ However, the methyl-rhodium complex, B, was never detected, and the first product observed from a stoichiometric oxidative addition of MeI to A was the acetyl complex C.⁶

We now report that, when the oxidative addition of MeI to Rh(CO)₂I₂⁻ is carried out in neat MeI solvent, the crucial intermediate MeRh(CO)₂I₃⁻, B, can be detected at low concentration using FTIR and FTNMR spectroscopy. The observation of B has also allowed estimation of the rate of the key methyl migration

(1) (a) Sheffield University. (b) BP Chemicals, Hull.

(2) Dekleva, T. W.; Forster, D. *Adv. Catal.* 1986, 34, 81.

(3) (a) Murphy, M.; Smith, B.; Torrence, G.; Aguilo, A. *Inorg. Chim. Acta* 1985, 101, 147; (b) *J. Organomet. Chem.* 1986, 303, 257; (c) *J. Mol. Catal.* 1987, 39, 115.

(4) (a) Schrod, M.; Luft, G. *Ind. Eng. Chem. Prod. Res. Dev.* 1981, 20, 649. (b) Schrod, M.; Luft, G.; Grobe, J. *J. Mol. Catal.* 1983, 20, 175. (c) Luft, G.; Schrod, M. *J. Mol. Catal.* 1983, 22, 169.

(5) Fulford, A.; Hickey, C. E.; Maitlis, P. M. *J. Organomet. Chem.* 1990, 398, 311. Hickey, C. E.; Maitlis, P. M. *J. Chem. Soc., Chem. Commun.* 1984, 1609.

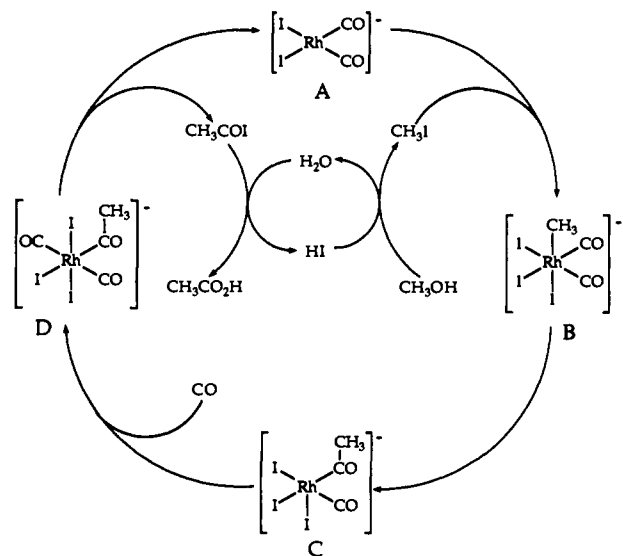
(6) The X-ray structure determination shows the acetyl complex C to be dinuclear in the solid with 6-coordinate Rh(III) and bridging iodides; Adanson, G. W.; Daly, J. J.; Forster, D. *J. Organomet. Chem.* 1974, 71, C17.

(12) Walsh, C. T.; Liu, J.; Rusnak, F.; Sakaitani, M. *Chem. Rev.* 1990, 90, 1105–1129.

(13) Thorneley, R. N. F.; Lowe, D. J. *Biochem. J.* 1983, 215, 393–403.

(14) Massey, V.; Hemmerich, P. *Biochemistry* 1978, 17, 9–17.

(15) Deistung, J.; Thorneley, R. N. F. *Biochem. J.* 1986, 239, 69–75.

Scheme 1. Cycle for the Rhodium and Iodide Catalyzed Carbonylation of Methanol to Acetic Acid²**Table I.** Kinetic and Absorbance Ratio Data for the Reaction of $\text{Bu}_4\text{N}[\text{Rh}(\text{CO})_2\text{I}_2]$ with Neat MeI ^a

$T, ^\circ\text{C}$	$10^4 k_{\text{obsd}}, \text{s}^{-1}$	$10^3 R_a$	$10^2 k_2, \text{s}^{-1}$
5.0	1.09	10.5	0.73
15.0	2.24	8.4	1.9
25.0	4.69	7.0	4.7
35.0	9.78	5.9	11.6

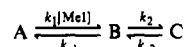
^a k_{obsd} is the pseudo-first-order rate constant for the overall reaction $\text{A} \rightarrow \text{C}$ (uncertainties, $\pm 0.1 \times 10^{-4}$ in k_{obsd} , $\pm 0.05 \times 10^{-3}$ in R_a).

(C–C bond-forming) step, $\text{B} \rightarrow \text{C}$.

A high steady-state ratio of the concentrations $[\text{B}]/[\text{A}]$ will be favored by a high $[\text{MeI}]$.⁷ For other systems it has previously been found that the rate of migration of methyl onto CO can be enhanced by factors of more than 10^4 in very polar solvents.⁸ Thus the use of a less polar solvent such as MeI should also favor detection of B by reducing the rate of the step $\text{B} \rightarrow \text{C}$.

The initial IR bands due to *cis*- $\text{Rh}(\text{CO})_2\text{I}_2^-$ [$\nu(\text{CO})$ 1985 and 2055 cm^{-1}] in a solution of $\text{Bu}_4\text{N}[\text{Rh}(\text{CO})_2\text{I}_2]$ in neat MeI⁹ were slowly replaced by those of the product C [$\nu(\text{CO})$ 1740, 2061 cm^{-1}]. However, careful observation consistently showed the presence of another small band, $\nu(\text{CO})$ 2104 cm^{-1} , in the region expected for the high-frequency band of B.^{10,11} During the reaction the 2104- cm^{-1} absorption decayed in direct proportion to the 1985- cm^{-1} band, due to A. It was also shown that the ratio of the absorptions, $A_{2104}/A_{1985} = R_a$, was directly proportional to $[\text{MeI}]$ over the range 12–16 M in dichloromethane at 25 $^\circ\text{C}$. Thus the 2104- cm^{-1} absorption behaved exactly as predicted for

(7) For the reaction scheme



assuming that k_{-2} is negligible, since the reaction $\text{A} \rightarrow \text{C}$ reaches completion, the steady-state approximation for $[\text{B}]$ gives the relationships

$$\frac{[\text{B}]}{[\text{A}]} = \frac{k_1[\text{MeI}]}{k_{-1} + k_2} \quad \text{and} \quad k_{\text{obsd}} = \frac{k_1 k_2 [\text{MeI}]}{k_{-1} + k_2}$$

where k_{obsd} is the pseudo-first-order rate constant for the reaction $\text{A} \rightarrow \text{C}$.

(8) See, for example: Mawby, R.; Basolo, F.; Pearson, R. G. *J. Am. Chem. Soc.* **1964**, *86*, 3994. Butler, I. S.; Basolo, F.; Pearson, R. G. *Inorg. Chem.* **1967**, *6*, 2077.

(9) **WARNING:** Both methyl iodide and the rhodium carbonyl complexes are extremely toxic! Special precautions need to be taken in working with them, especially when MeI is used a solvent!

(10) A *cis*-dicarbonyl structure would be expected to exhibit two $\nu(\text{CO})$ bands of similar intensity. It is likely that the low-frequency band is hidden by the absorptions of A and C near 2060 cm^{-1} .¹¹

(11) These data compare well with those reported for the analogous iridium system: $\text{MeIr}(\text{CO})_2\text{I}_3^-$ [$\nu(\text{CO})$ 2049, 2102 cm^{-1}], $\text{Ir}(\text{CO})_2\text{I}_2^-$ (1970, 2045 cm^{-1}). Forster, D. *Inorg. Nucl. Chem. Lett.* **1969**, *5*, 433; *Inorg. Chem.* **1972**, *11*, 473.

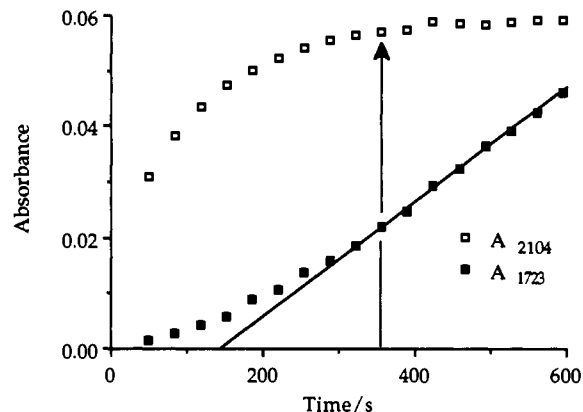


Figure 1. Graph showing the behavior of the IR bands due to species B (2104 cm^{-1}) and species C (1723 cm^{-1}) in the first 10 min of the reaction of $\text{Bu}_4\text{N}[\text{Rh}(\text{CO})_2\text{I}_2]$ (0.1 M) with neat CH_3I at 5 $^\circ\text{C}$. Note that the rate of formation of species C and the concentration of species B both reach a maximum after ca. 6 min (indicated by the arrow). The best straight-line fit for the 1723- cm^{-1} data between 6 and 10 min is also shown.

B by the steady-state approximation.⁷ The ratio R_a was larger at lower temperatures (Table I).

Monitoring the reaction at 5 $^\circ\text{C}$ revealed that the 2104- cm^{-1} absorption did not attain its maximum intensity until ca. 6 min after mixing (Figure 1). A first-order rate constant of $8.5 \pm 0.5 \times 10^{-3} \text{ s}^{-1}$ was measured for the appearance of B, corresponding to a $t_{1/2}$ of ca. 80 s. Thereafter the absorption decays at the same rate as that of A at 1985 cm^{-1} ; the rate of formation of species C does not reach a peak until the 2104- cm^{-1} band reaches the maximum intensity. This is the expected behavior for a band belonging to B since the predicted dependence is $d[\text{C}]/dt = k_2[\text{B}]$.

This interpretation of the IR data was confirmed by low-temperature $^{13}\text{C}\{^1\text{H}\}$ NMR spectroscopy using ^{13}C -enriched reactants. A solution of $\text{Bu}_4\text{N}[\text{Rh}(\text{CO})_2\text{I}_2]$ in $^{13}\text{C}_3\text{H}_8$ ¹² was made up at -60 $^\circ\text{C}$ and transferred to the probe of a Bruker WH400 NMR spectrometer at -50 $^\circ\text{C}$. The only new signals observed on addition of the rhodium salt were those arising from natural abundance ^{13}C in the $\text{Bu}_4\text{N}[\text{Rh}(\text{CO})_2\text{I}_2]$. When the sample was briefly warmed to $+20$ $^\circ\text{C}$, to allow reaction, and then returned to the -50 $^\circ\text{C}$ NMR probe, a new doublet was observed in the rhodium methyl region [$\delta(^{13}\text{C})$ -0.65 ppm, $^1J(^{103}\text{Rh}-^{13}\text{C}) = 14.7$ Hz] as well as signals due to a small amount of species C.¹³ With the H decoupler switched off, the rhodium–methyl signal was split into a quartet of doublets, with $^1J(^{13}\text{C}-^1\text{H}) = 143$ Hz, the same as in $\text{MeRh}(\text{PPh}_3)_2\text{I}_2$.¹⁴ A value of δ 2.08 ppm for the ^1H resonance of the methyl of B was found indirectly from the ^{13}C NMR spectrum;^{15,16} this is again typical of a methyl–rhodium species. The sample was warmed until conversion of A into C was complete, when the doublet at δ -0.65 could no longer be observed.

Similar experiments using ca. 70% ^{13}C enriched $\text{Bu}_4\text{N}[\text{Rh}(\text{CO})_2\text{I}_2]$ in unenriched MeI enabled assignment of a doublet (δ 175.1 ppm, $^1J(^{103}\text{Rh}-^{13}\text{C}) = 60$ Hz) to the terminal carbonyls of B, suggesting strongly that they are equivalent. Coupling between the methyl and carbonyl ^{13}C signals of B could not be detected in an experiment using ^{13}C -enriched samples of both $\text{Rh}(\text{CO})_2\text{I}_2^-$ and MeI. However, only a very small $^2J(^{13}\text{C}-^{13}\text{C})$ is expected

(12) Containing 99% ^{13}C , from Aldrich; 10% $(\text{CD}_3)_2\text{CO}$ was added as a lock signal. Separate tests showed that the acetone had no effect.

(13) At $\delta(^{13}\text{C})$ 48.64, 49.76 ppm, arising from the methyls of two isomers: Bailey, N. A.; Mann, B. E.; Manuel, C. P.; Spencer, C. M.; Kent, A. G. *J. Chem. Soc., Dalton Trans.* **1988**, 489.

(14) Siedle, A. R.; Newmark, R. A.; Pignolet, L. H. *Organometallics* **1984**, *3*, 855.

(15) The ^1H chemical shift was determined using off-resonance decoupling at various frequencies,¹⁶ since this technique is far faster than two-dimensional $^{13}\text{C}-^1\text{H}$ correlation for a single ^{13}C group. The ^1H signal could not be detected directly due to its proximity to the intense $^{13}\text{CH}_3$ signal.

(16) Archer, R. A.; Cooper, R. D. G.; Demarco, P. V.; Johnson, L. R. F. *J. Chem. Soc., Chem. Commun.* **1970**, 1291. Wehrli, F. W.; Wirthlin, T. *Interpretation of Carbon-13 NMR spectra*; Heyden: London, 1978; p 69.

if B has the fac stereochemistry depicted in Scheme 1.

A combination of kinetic data for the conversion of A to C with estimated values of $[B]/[A]$ has allowed estimation of the rate of methyl migration (k_2). An Arrhenius plot of the data in Table I over the range 5–35 °C yielded a good straight line (correlation coefficient 0.999) and gave activation parameters of $\Delta H^\ddagger = 63 \pm 2 \text{ kJ mol}^{-1}$ and $\Delta S^\ddagger = -59 \pm 9 \text{ J mol}^{-1} \text{ K}^{-1}$ for the crucial methyl migration (carbonylation) step of the catalytic cycle.¹⁷

These data show that oxidative addition of MeI to A proceeds normally to give a methyl-rhodium complex B. The large values obtained for k_2 show that the previous nonobservation of B is due primarily to the rapidity with which it reacts to give species C. High rates of alkyl migration have been reported for other rhodium systems,¹⁸ much faster than for other unactivated metals in nonpolar solvents.⁸ This is probably the major reason why rhodium is such a good carbonylation catalyst.

Acknowledgment. We thank BP Chemicals, the SERC, and the University of Sheffield for generous support of this work, NATO (Grant CRG 900289) for a travel award, and Johnson Matthey for the loan of some rhodium chloride.

Registry No. B, 136358-08-2; $\text{Bu}_4\text{N}[\text{Rh}(\text{CO})_2\text{I}_2]$, 30192-00-8.

Supplementary Material Available: Experimental details including a warning on the extreme toxicity of methyl iodide and the rhodium carbonyl complexes (2 pages). Ordering information is given on any current masthead page.

(17) The values for the overall reaction, $\text{A} + \text{MeI} \rightarrow \text{C}$, in neat MeI are $\Delta H^\ddagger = 50 \text{ kJ mol}^{-1}$ and $\Delta S^\ddagger = -142 \text{ J mol}^{-1} \text{ K}^{-1}$, giving a ΔG^\ddagger_{298} of 92 kJ mol^{-1} compared with a ΔG^\ddagger_{298} of 79 kJ mol^{-1} for the methyl migration $\text{B} \rightarrow \text{C}$.

(18) Bassetti, M.; Sunley, G. J.; Fanizzi, F. P.; Maitlis, P. M. *J. Chem. Soc., Dalton Trans.* 1990, 1799. Douek, Z.; Wilkinson, G. *J. Chem. Soc. A* 1969, 2604. Bennett, M. A.; Jeffery, J. C.; Robertson, G. B. *Inorg. Chem.* 1981, 20, 323.

Two-State Propagation Mechanism for Propylene Polymerization Catalyzed by *rac*-[*anti*-Ethylidene(1- η^5 -tetramethylcyclopentadienyl)(1- η^5 -indenyl)]dimethyltitanium

James C. W. Chien,^{*1a,b} Geraldo Hidalgo Llinas,^{1a} Marvin D. Rausch,^{1b} G.-Y. Lin,^{1c} and H. Henning Winter^{1c}

Departments of Polymer Science and Engineering, Chemistry, and Chemical Engineering
University of Massachusetts
Amherst, Massachusetts 01003

Jerry L. Atwood and Simon G. Bott

Department of Chemistry, University of Alabama
Tuscaloosa, Alabama 35487
Received June 17, 1991

ansa-Metallocene compounds with local C_2 symmetry have been actively investigated as catalysts for the isospecific polymerization of propylene.²⁻⁴ Recently, we reported that the nonsymmetric *rac*-[ethylidene(1- η^5 -tetramethylcyclopentadienyl)(1- η^5 -indenyl)]dichlorotitanium/methylaluminoxane (**1**/MAO) catalyst⁵

(1) (a) Department of Polymer Science and Engineering. (b) Department of Chemistry. (c) Department of Chemical Engineering.

(2) (a) Ewen, J. A. *J. Am. Chem. Soc.* 1984, 106, 6355. (b) Ewen, J. A. In *Catalytic Polymerization of Olefins*; Keii, T., Soga, K., Eds.; Elsevier: New York, 1986; p 271. (c) Ewen, J. A.; Haspeslagh, L.; Atwood, J. L.; Zhang, H. *J. Am. Chem. Soc.* 1987, 109, 6544.

(3) Kaminsky, W.; K lper, K.; Brintzinger, H. H.; Wild, F. R. W. P. *Angew. Chem., Int. Ed. Engl.* 1985, 24, 507.

(4) (a) Rieger, B.; Chien, J. C. W. *Polym. Bull.* 1989, 21, 159. (b) Rieger, B.; Mu, X.; Mallin, D. T.; Rausch, M. D.; Chien, J. C. W. *Macromolecules* 1990, 23, 3559. (c) Chien, J. C. W.; Sugimoto, R. *J. Polym. Sci., Part A* 1991, 29, 459.

(5) Mallin, D. T.; Rausch, M. D.; Lin, Y.-G.; Dong, S.-H.; Chien, J. C. W. *J. Am. Chem. Soc.* 1990, 112, 2030.

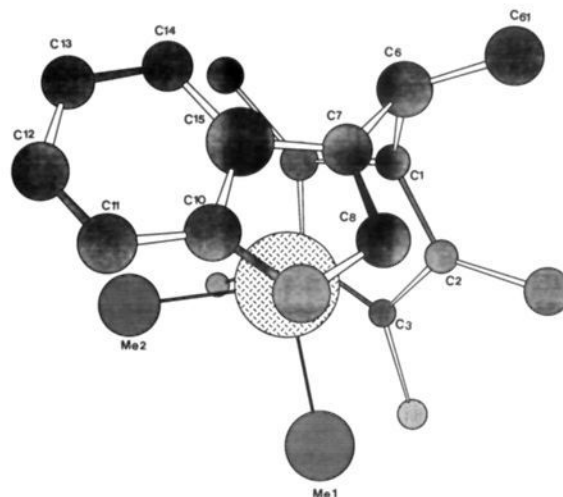


Figure 1. Molecular structure and atom-numbering scheme of *rac*-[ethylidene(1- η^5 -tetramethylcyclopentadienyl)(1- η^5 -indenyl)]dimethyltitanium (**2**). Important interatomic distances (Å) and bond angles (deg) are as follows: Ti–Me(1), 2.08 (1); Ti–Me(2), 2.00 (1); Ti–C(1), 2.21 (1); Ti–C(2), 2.32 (1); Ti–C(3), 2.44 (1); Ti–C(4), 2.47 (1); Ti–C(5), 2.37 (1); Ti–C(7), 2.10 (1); Ti–C(8), 2.17 (1); Ti–C(9), 2.41 (1); Ti–C(10), 2.56 (1); Ti–C(15), 2.40 (1); Ti–CEN(1), 2.07 (1); Ti–CEN(2), 2.01 (1); CEN(1)–Ti–CEN(2), 126.983; Me(1)–Ti–Me(2), 101.2 (5); CEN(1)–Ti–Me(1), 107.9 (4); CEN(2)–Ti–Me(1), 106.5 (3); CEN(1)–Ti–Me(2), 108.5 (4); CEN(2)–Ti–Me(2), 102.8 (3); C(1)–C(6)–C(7), 105.4 (9). [CEN(1) is centroid of C(1)–C(5); CEN(2) is centroid of C(7)–C(10) and C(15).]

produced stereoblock macromolecular chains comprising alternating sequences of stereoregular, crystallizable (*cry*) and stereoirregular, amorphous (*am*) polypropylene (PP),^{5,6} i.e., a thermoplastic elastomer (TPE-PP). We proposed that the catalytic species can exist in two interconverting states polymerizing propylene stereoselectively by one state, but nonselectively by the other state. We now report the synthesis, structure, and polymerization behavior of the title compound (**2**). The properties of **2** provide strong support for the proposed two-state propagation mechanism.

Compound **2** was synthesized by reacting a suspension of **1**⁷ in *n*-hexane with **2** equiv of methylolithium. After filtration, concentration, and cooling at –20 °C, orange red crystals of **2** were obtained in 60% yield. Anal. Found (calcd): C, 77.2 (77.66); H, 8.18 (8.23). The ¹H NMR spectrum of **2**⁸ showed two singlets for the nonequivalent methyl groups bonded to titanium at –1.09 ppm and 0.17 ppm.

Crystals of **2** suitable for the X-ray diffraction study were grown by the slow cooling of a hexane solution of **2** at –20 °C. The space group was found to be $P2_1/c$, and the unit cell parameters are $a = 11.220$ (1) Å, $b = 9.366$ (2) Å, $c = 18.470$ (3) Å; $\beta = 106.75$ (1)°; and $D_{\text{calcd}} = 1.22 \text{ g cm}^{-3}$ for $Z = 4$. Least-squares refinement based on 729 observed reflections produced the final discrepancy indices $R = 0.054$ and $R_w = 0.056$.

The methyl group attached to the bridging carbon atom in **2** is oriented in an anti arrangement relative to the six-membered ring of the indenyl ligand (Figure 1). The two σ -bonded methyl substituents are located in sterically nonequivalent positions, with Me(2) oriented toward the six-membered ring of the indenyl ligand. Furthermore, the Ti–CH₃ distances are significantly different, with Ti–Me(1) = 2.08 (1) Å and Ti–Me(2) = 2.00 (1) Å.⁹

(6) Chien, J. C. W.; Llinas, G. H.; Dong, S.-H.; Winter, H. H.; Lin, G.-Y.; Rausch, M. D. *Macromolecules*, submitted.

(7) Reaction of [ethylidene(1- η^5 -tetramethylcyclopentadienyl)(1- η^5 -indenyl)]dilithium with $\text{TiCl}_4 \cdot 2\text{THF}$ gave **1** as the sole product. Under the same conditions, the reaction with TiCl_4 produced an equimolar mixture of **1** and its syn diastereomer.

(8) ¹H NMR spectrum (C_6D_6): –1.09 (s, 3 H), 0.17 (s, 3 H) for TiCH_3 ; 1.36 (s, 3 H), 1.50 (s, 3 H), 1.91 (s, 3 H), 1.95 (s, 3 H) for CH_3 of Cp*; 1.54 (d, 3 H) for ethylidene CH_3 ; 3.84 (q, 1 H) for ethylidene H; and 5.22 (d, 1 H), 6.88 (m), 7.68 (m), 7.20 (m) for the aromatic H of indenyl.